THE JOURNAL OF PHYSICAL CHEMISTRY LETTERS
A JOURNAL OF THE AMERICAN CHEMICAL SOCIETY

pubs.acs.org/JPCL Letter

Minimizing the Time-Dependent Density Functional Error in Ehrenfest Dynamics

Lionel Lacombe* and Neepa T. Maitra*

Cite This: *J. Phys. Chem. Lett.* 2021, 12, 8554−8559 Read Online

ACCESS | Metrics & More | Article Recommendations | Supporting Information

ABSTRACT: Simulating electron−ion dynamics using time-dependent density functional theory within an Ehrenfest dynamics scheme can be done in two ways that are in principle exact and identical: propagating time-dependent electronic Kohn−Sham equations or propagating electronic coefficients on surfaces obtained from linear-response. We show here that using an approximate functional leads to qualitatively different dynamics in the two approaches. We argue that the latter is more accurate because the functionals are evaluated on domains close to the ground state where currently used approximations perform better. We demonstrate this on an exactly solvable model of charge transfer and discuss implications for time-resolved spectroscopy.

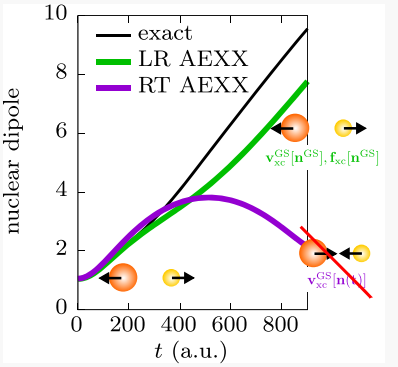

Coupled electron−nuclear dynamics lies at the heart of several topical phenomena, including photovoltaic design, photocatalysis, and the laser control of chemical reactions. To accurately simulate these processes computationally, adequate accounting of both electron−nuclear correlation as well as electron−electron interactions is needed in practical dynamics schemes. From the purely electronic structure side, time-dependent density functional theory (TDDFT)[1−4] is a practical choice when more than a few atoms are involved: one solves a system of noninteracting electrons, the Kohn−Sham system, in which many-body interaction effects are "hidden" in the exchange−correlation (xc) functional. TDDFT has yielded useful agreement with experiment in an impressive array of cases, including when coupled to nuclear motion.[5−7] From the electron−nuclear coupling side, the mixed quantum−classical methods of Ehrenfest dynamics and trajectory surface-hopping are currently most widely used. While Ehrenfest dynamics is unable to capture effects like wavepacket splitting, it has several desirable features that make it more attractive to use in many cases, including that it is cheaper and faster because it is does not rely on a stochastic algorithm, which enables calculations on large systems (see e.g. ref 8 for a computation involving 59 400 electrons). Furthermore, it is derivable from first principles and so does not have to make somewhat *ad hoc* choices such as velocity-rescaling that surface-hopping does.

TDDFT is an ideal partner for Ehrenfest dynamics because the coupling of the electronic system to the nuclear one is directly via the electronic density, so no additional "observable functionals"[4] need to be extracted from the Kohn−Sham system. It is available in several widely used codes, such as Octopus,[9] NWChem,[10] Quantum Espresso,[11] Salmon,[12] Siesta,[13] or CPMD,[14] where it is implemented in one of two distinct ways: one involving propagation of time-dependent Kohn−Sham orbitals, and the other propagation of coefficients involving energies and couplings obtained from TDDFT linear response. When using the same approximate functional, one would hope to get similar results from the different codes, all else (e.g., basis sets, convergence thresholds) being the same. However, we show here that the two distinct implementations lead to qualitative differences in the resulting dynamics. Fundamentally, this is because the domains that the xc functional is evaluated on are fundamentally different. One implementation probes the functional on the fully non-equilibrium time-dependent density, and the true and KS wave functions underlying the density at any time are typically not ground states. The other implementation needs to evaluate it and its functional derivative merely on a density whose underlying state is a ground state at the instantaneous nuclear configuration. Because approximate functionals tend to be more accurate in the latter case, the resulting Ehrenfest dynamics is also much more accurate when the implementation is done in this way. We demonstrate this explicitly on a model system of photoexcited charge transfer where a comparison with exact dynamics can be made. We discuss the significance of these results for time-resolved spectroscopy.

Received: June 23, 2021
Accepted: August 20, 2021

https://doi.org/10.1021/acs.jpclett.1c02020
J. Phys. Chem. Lett. 2021, 12, 8554−8559

In Ehrenfest dynamics,[15] the nuclei are described by an ensemble of classical trajectories evolving on an averaged potential energy surface (PES) determined by the electrons:

$$M_\nu \ddot{\mathbf{R}}_\nu^{(I)} = -\langle \Psi^{(I)} | \nabla_\nu H_{\mathrm{BO}} | \Psi^{(I)} \rangle \tag{1}$$

where $\Psi^{(I)}$ is the electronic wave function following the electronic TDSE, $H_{\mathrm{BO}}(R^{(I)}(t))\Psi^{(I)} = i\partial_t \Psi^{(I)}$, with the instantaneous position of trajectory I appearing in the electron−nuclear coupling term in the Born−Oppenheimer (BO) Hamiltonian, $H_{\mathrm{BO}} = T_e + V$, where T_e is the electronic kinetic energy operator and V includes all potentials. Noting that the nuclear gradient operates only on the electron−nuclear interaction potential, $V_{en} = \sum_n^{N_e}\sum_\nu^{N_n} v_{en}(|\mathbf{r}_n - \mathbf{R}_\nu|)$, which is a multiplicative one-body operator from the standpoint of the electrons, we may rewrite this as

$$M_\nu \ddot{\mathbf{R}}_\nu = -\int \mathrm{d}^3 r n(\mathbf{r}, t) \nabla_\nu V_{en}(\underline{\mathbf{r}}, \underline{\underline{\mathbf{R}}}) - \nabla_\nu V_{nn}(\underline{\underline{\mathbf{R}}}) \tag{2}$$

where $n(\mathbf{r}, t) = N\sum_\sigma \int \mathrm{d}^3 r_2 ... d^2 r_N |\Psi(\mathbf{r}, \mathbf{r}_2, ..., \mathbf{r}_N)|^2$ is the one-body electron density and $\underline{\mathbf{r}}$ and $\underline{\underline{\mathbf{R}}}$ denote coordinates of all the electrons and nuclei, respectively. The problem then appears perfectly suited to work with TDDFT, where, instead of having to solve a many-body interacting TDSE, the $n(\mathbf{r}, t)$ is produced by evolving one-body TDKS equations[1−3]

$$(-\nabla^2/2 + v_S(\mathbf{r}, t))\phi_k(\mathbf{r}, t) = i\partial_t \phi_k(\mathbf{r}, t) \tag{3}$$

with $n(\mathbf{r}, t) = \sum_{k\in \mathrm{occ.}} |\phi_k(\mathbf{r}, t)|^2$ and

$$v_S(\mathbf{r}, t) = v_{en}(\mathbf{r}, \underline{\underline{\mathbf{R}}}^{(I)}(t)) + v_H[n](\mathbf{r}, t) + v_{\mathrm{XC}}[n; \Psi_0, \Phi_0](\mathbf{r}, t) \tag{4}$$

Atomic units are used throughout this paper. Here $v_H[n](\mathbf{r}, t) = \int \frac{n(\mathbf{r}', t)}{|\mathbf{r} - \mathbf{r}'|} d^3 r'$ is the Hartree potential, and v_{XC} is the xc potential, in principle a functional of the initial interacting state Ψ_0, the initial choice of KS orbitals Φ_0, and the history of the density. Armed with an approximation for v_{XC}, eqs 2−4 are solved together, with the electronic and nuclear dynamics coupled through the electronic density and nuclear position, and we refer to this approach as "real-time (RT) Ehrenfest".

It is equivalent to instead expand $|\Psi(t)\rangle$ in terms of the exact interacting BO eigenstates and evolve the coefficients: writing $|\Psi^{(I)}(t)\rangle = \sum_j C_j(t) |\Psi^{\mathrm{BO}}_{\underline{\underline{\mathbf{R}}}^{(I)}(t), j}\rangle$, where $H_{\mathrm{BO}}\Psi^{\mathrm{BO}}_{\underline{\underline{\mathbf{R}}}, j} = E_j(\underline{\underline{\mathbf{R}}})\Psi^{\mathrm{BO}}_{\underline{\underline{\mathbf{R}}}, j}$ we have

$$\dot{C}_j^{(I)}(t) = -iE_j^{(I)}(t)C_j^{(I)}(t) - \sum_\nu \sum_k \mathbf{d}^{(I)}_{\mathrm{jk},\nu} \cdot \dot{\mathbf{R}}_\nu^{(I)} C_k^{(I)} \tag{5}$$

using the short-hand $E_j^{(I)}(t) = E_j(\underline{\underline{\mathbf{R}}}^{(I)}(t))$ and the nonadiabatic couplings $\mathbf{d}_{jk,\nu} = \langle \Psi_j^{\mathrm{BO}} | \nabla_\nu \Psi_k^{\mathrm{BO}} \rangle$. In terms of these coefficients, the force on the nuclei takes the form of the weighted average

$$M_\nu \ddot{\mathbf{R}}_\nu^{(I)} = -\sum_j |C_j^{(I)}(t)|^2 \nabla_\nu E_j^{(I)}(t) - \sum_{jk} C_j^{(I)*}(t) C_k^{(I)}(t)(E_k^{(I)}(t) - E_j^{(I)}(t))\mathbf{d}^{(I)}_{\mathrm{jk},\nu} \tag{6}$$

Equations 5 and 6 present an alternative implementation of Ehrenfest dynamics and can also be used in conjunction with TDDFT, where linear response gives the energies $E_j(R)$ and couplings $\mathbf{d}_{jk,\nu}$ between ground and excited states, with quadratic response giving the couplings between excited states.[16−18] We denote the approach eqs 5 and 6 as "linear-response (LR) Ehrenfest".

In theory, the RT-Ehrenfest scheme (eqs 2−4) and the LR-Ehrenfest scheme (eqs 5 and 6) are entirely equivalent, and if the exact functionals were known and used, they would yield identical results for both electronic and nuclear observables, corresponding to running Ehrenfest dynamics with an exact electronic structure method.

However, in practice, there is a fundamental difference due to the domains on which the xc functionals in the two approaches are evaluated. While LR-Ehrenfest requires functionals for the xc energy and xc kernel evaluated on the density obtained from a ground state, RT-Ehrenfest requires the functional for the xc potential to be evaluated on the fully nonequilibrium time-dependent density where the underlying states of the true system and KS system are far from any ground state. Because functional approximations in use today are predominantly adiabatic, i.e. built from ground-state ones, they tend to perform much better in the LR regime than in nonperturbative situations, and so we expect that the LR-Ehrenfest scheme will give more reliable and accurate results than the RT-Ehrenfest scheme.

This situation is not dissimilar to TDDFT simulations of the purely electronic scattering problem[19] where a time-resolved calculation of electron−molecule scattering dynamics probes the xc functional in a fully nonlinear regime, giving far poorer scattering probabilities than a formulation extracting these same probabilities from linear response. Although the response-based formulation is valid only in the elastic case and cannot provide a time-resolved picture, the results in the elastic case are better than in the real-time calculation.

Returning to the electron−ion dynamics, we note that the difference between the two schemes persists even when there is negligible nonadiabatic coupling such that Ehrenfest reduces to BO. That is, even in cases where dynamics is such that the nuclear trajectories evolve on a single excited BO PES, the LR-BO and RT-BO methods will give different answers when the same approximate functional is used. They will agree only when the dynamics takes place on purely the ground-state PES.

We use an exactly solvable model system simulating a photoexcited ion-driven charge-transfer event to explicitly demonstrate the problem. Consider a one-dimensional molecule consisting of two soft-Coulomb interacting electrons, an ion with net charge $Z = 2$ and mass $m_1 = 2m_p$ and an atom of zero net charge and mass $m_2 = 6m_p$, with $m_p = 1836.1528$ au being the mass of the proton. The ion may be thought of as a bare nucleus, and its interaction with the electrons is taken as soft-Coulomb. The atom may be thought of as a nucleus surrounded by a frozen cloud of electrons, such that it presents a short-ranged screened soft-Coulomb potential to the electrons. The ion-atom is also taken as screened soft-Coulomb; details are given in the Supporting Information. In the dissociation limit, the ground state captures both electrons in the soft-Coulomb well, while the first excited state represents a charge-transfer state with one electron in the ionic well and the other in the atomic well. Figure 1 shows these two BO states, as well as the lowest three BO PESs as a function of ion−atom separation R. We show also the surfaces obtained from DFT and LR TDDFT using two contrasting functional approximations: adiabatic local density approximation (ALDA),[20,21] which has local dependence on the density in time and in space, and adiabatic exact exchange (AEXX), which has a nonlocal dependence on the density in space but is still local in time. In this two-electron case, for AEXX $v_X[n](\mathbf{r}, t) = -v_H[n](\mathbf{r}, t)/2$. We observe that they both

https://doi.org/10.1021/acs.jpclett.1c02020
J. Phys. Chem. Lett. 2021, 12, 8554−8559

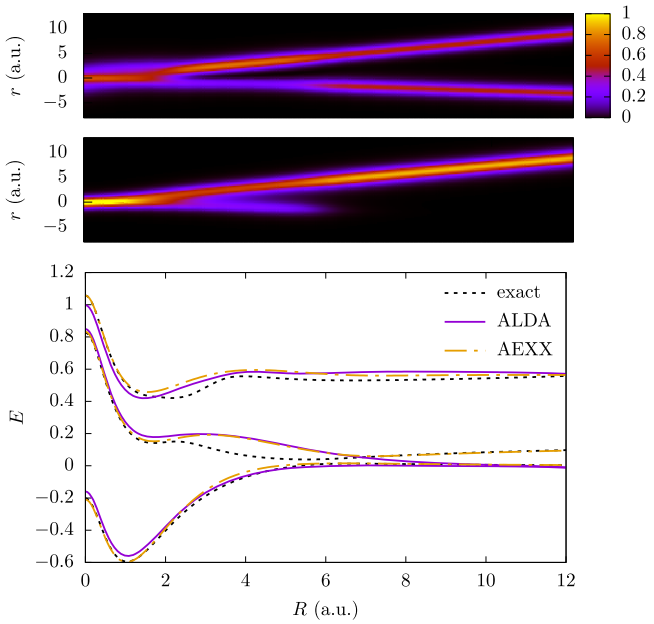

Figure 1. Lowest three singlet BO PESs, exact, linear-response ALDA, and AEXX BO PESs as indicated in the legend (lower panel). Heat map of exact electronic BO wave function $|\Psi^{BO}_{R,0}(r)|^2$ (middle panel) and same for $|\Psi^{BO}_{R,1}(r)|^2$ (upper panel).

approximate the ground-state energy quite well for all R. For large R, AEXX captures the asymptotic $I_D - A_A - 1/R$ tail of the exact charge-transfer state well, while ALDA collapses to zero, as expected.[22] The ALDA ground and first excited orbitals become degenerate and delocalized over the molecule. At intermediate distances, we see that ALDA and AEXX excited BO PESs are very similar to each other, with a more pronounced shape resonance than the exact.

The eigenvectors of the TDDFT linear response matrix indicate that the first excitation is so significantly dominated by the lowest KS excitation that a small matrix approximation[2,23,24] yields practically the same curves for both functional approximations; higher excited states mix in negligibly. The density of the excited state is then very well-approximated by the density of the KS excited determinant, which will ease our task in finding the electronic dipole and densities from LR-Ehrenfest calculations.

We now begin the dynamics from an initial Franck−Condon photoexcitation to the first excited electronic state: the initial state of the molecule is $\Psi^{mol}(r, R, 0) = \chi_0^{(0)}(R)\Psi^{BO}_{R,1}(r)$ where $\chi_0^{(0)}(R)$ denotes the nuclear ground state on the lowest BO surface. In the Ehrenfest calculations, we sample 100 initial positions and momenta from the initial Wigner phase space distribution of the ground nuclear wave function of the ground electronic surface. Due to the slope of the first excited surface, the nuclear wavepacket moves toward larger R but slowly enough such that as it passes the avoided crossing region around $R \approx 5.8$ au it remains largely in the excited state. Only a small fraction of the wavepacket transfers to the ground-state surface: in the exact dynamics, the maximum population of the ground BO state is 0.166 which then largely transfers back, leaving only 0.03 ground-state population at long times. In an Ehrenfest calculation using the exact surfaces, even less, 0.04, transfers to the lower surface near the avoided crossing, while at long times only 0.03 remains there. Thus, Ehrenfest dynamics practically reduces to BO dynamics on the first excited state. The exact nuclear dipole moment shown in Figure 2 agrees closely with that of a 100-trajectory RT-Ehrenfest calculation using forces

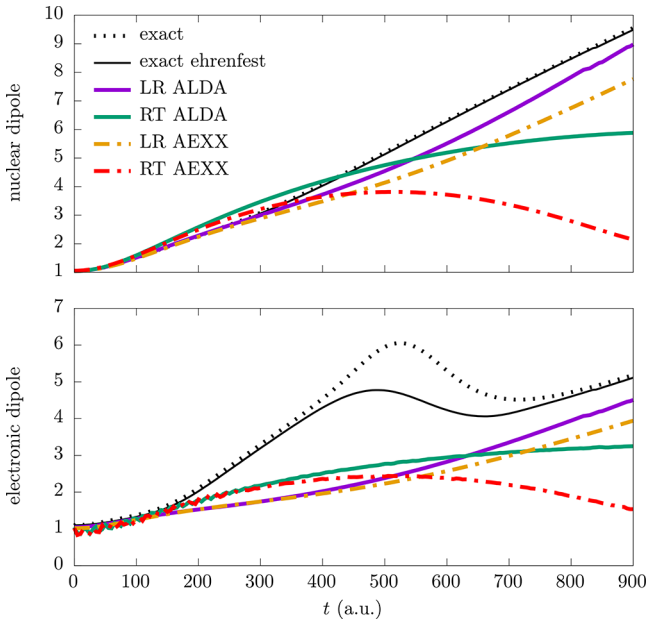

Figure 2. Time-dependent nuclear (upper panel) and electronic (lower panel) dipoles: exact, exact Ehrenfest, and the TDDFT LR-Ehrenfest and RT-Ehrenfest calculations; LR ALDA, RT ALDA, LR AEXX, and RT AEXX as indicated in the legend.

derived from the exact first BO surface, denoted "exact Ehrenfest". The lower panel shows the electronic dipoles are close except as the avoided crossing region is passed, where the exact density has a larger ground-state component than the Ehrenfest one, as noted above. The difference is less remarkable in the electronic densities (see Figure 3 and a movie in the Supporting Information).

Turning now to the TDDFT approximations shown in Figure 2 (with all Ehrenfest results obtained from the 100 trajectories), an immediate observation is the qualitatively incorrect behavior of the RT calculations for both the nuclear and electronic dipoles: after their initial rise, these curve downward, instead of continuing to move to larger values; ultimately, neither dissociate nor transfer the electron. The RT ALDA is a better approximation than the RT AEXX; this is also true for the electronic density shown in Figure 3 (see also a movie in the Supporting Information, which also shows the KS potentials for the two cases). The LR TDDFT calculations perform qualitatively much better, even if they undershoot both the nuclear and electronic dipoles, largely because of the wrong shape of the linear response curve in the intermediate region $R \approx 2-7$ au (Figure 1). Although at earlier times the error in the electronic dipole from the RT calculations is less than that in the LR ones, an inspection of the electronic densities in Figure 3 and in the movies provided in the Supporting Information shows that the RT densities are not better; the averaging inherent in the electronic dipole overweighs the large-r regions. Around $R = 5.8$ au the density of the exact first-excited state switches from being mainly localized on the ion to the 50:50 charge-transfer density, as evident in Figure 1 and reflected in the step in the exact and exact-Ehrenfest electronic dipole in Figure 2. On the other hand, the ALDA and AEXX excited-state densities do not have this feature, showing instead a smoother charge transfer and

https://doi.org/10.1021/acs.jpclett.1c02020
J. Phys. Chem. Lett. 2021, 12, 8554−8559

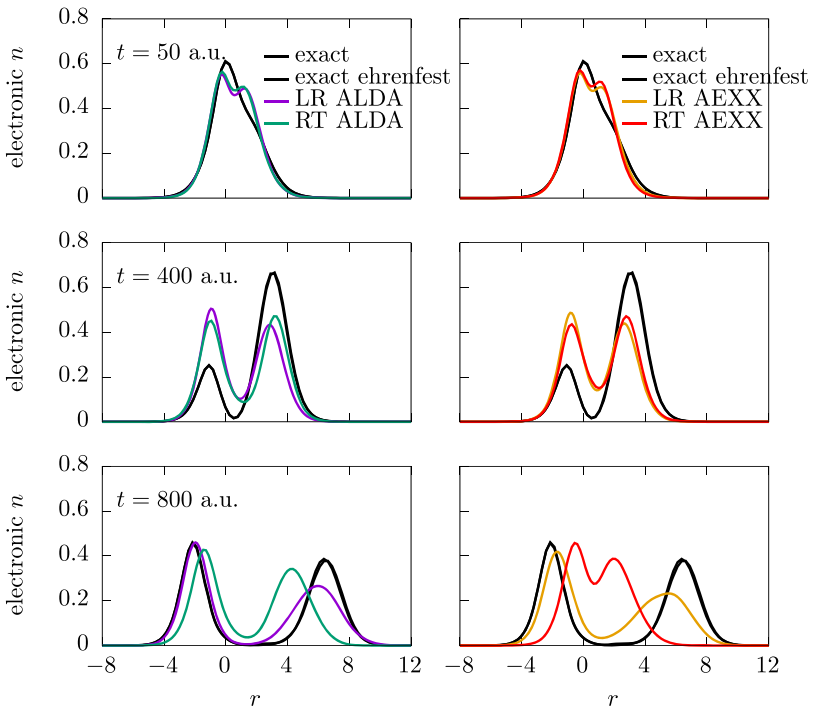

Figure 3. Snapshots of electronic densities for different times. Left column: exact (black dotted), exact-Ehrenfest (black solid), LR ALDA (violet solid), and RT ALDA (green solid). Right column: exact (black dotted), exact-Ehrenfest (black solid), LR AEXX (orange dash dotted), and RT AEXX (red dash dotted).

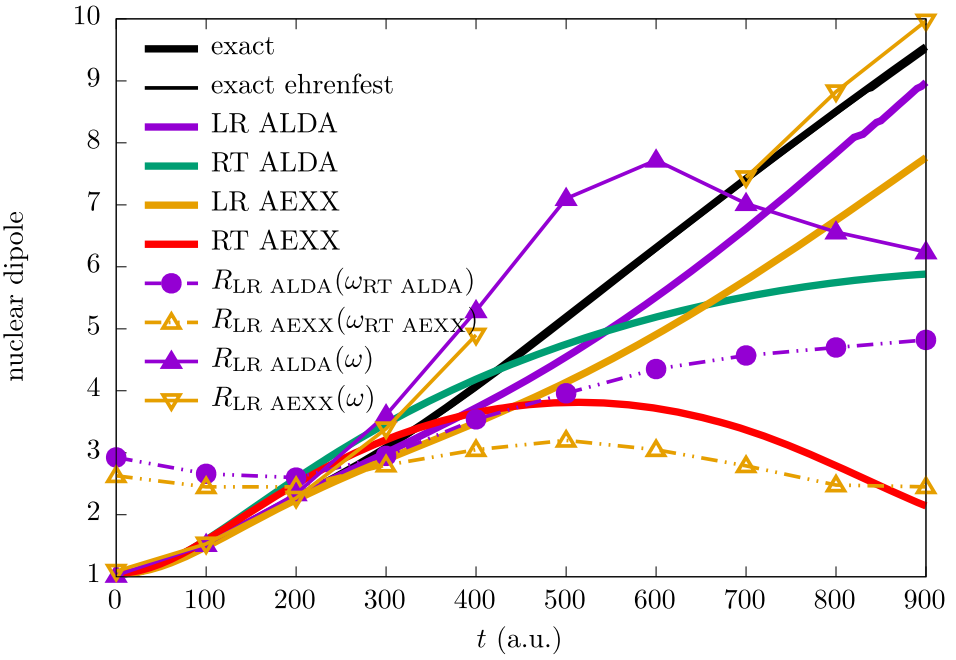

Figure 4. Deduced time-dependent nuclear dipole: $R_{\mathrm{LRALDA}}(\omega)$, $R_{\mathrm{LRAEXX}}(\omega)$, $R_{\mathrm{LRALDA}}(\omega_{\mathrm{RTALDA}})$, and $R_{\mathrm{LRAEXX}}(\omega_{\mathrm{RTAEXX}})$ compared with exact, exact Ehrenfest, RT ALDA, RT AEXX, LR ALDA, and LR AEXX with colors as indicated in the legend.

corresponding dipole. It appears the LR ALDA dipoles and densities are better than LR AEXX (except at large times where the LR ALDA nuclei move too fast because of the lack of the $-1/R$ tail); the LR ALDA benefits from a partial cancellation of errors in that the effect of the underestimated slope at intermediate time is compensated by the lack of the $-1/R$ at later times.

The fundamental reason that the LR-Ehrenfest dynamics is better than the RT can be understood from the earlier argument considering the domains of the xc functionals involved in the two types of calculations. The underlying assumption of an adiabatic approximation is that the exchange−correlation properties of the system are well-approximated by ground-state exchange−correlation, which is unlikely to be true for systems far from a ground state. In LR-Ehrenfest, the functionals

https://doi.org/10.1021/acs.jpclett.1c02020
J. Phys. Chem. Lett. 2021, 12, 8554−8559

are evaluated perturbatively away from a ground state, so adiabatic approximations are expected to perform better than when they are applied to the fully nonlinear density as they are in RT-Ehrenfest. Our results imply that when using TDDFT with adiabatic functionals, LR-Ehrenfest calculations are preferable to RT ones.

As a last, dramatic illustration of this, consider the application to femtosecond pump−probe spectroscopy set-ups, where the prospect of probing nuclear motion through electronic spectra has been raised.[25−27] The idea is that by comparing the measured time-resolved absorption spectrum of a molecule with the calculated spectrum at different nuclear configurations one can track the nuclear geometries as a function of time. If LR TDDFT is used to calculate the spectrum then Figure 4 plots the deduced nuclear separation $R_{\mathrm{LRTDDFT}}(\omega)$ where $\omega = \omega(t)$ is the time-resolved excitation energy of the molecule at time t. That is, we plot the R_{LRTDDFT} that satisfies $\omega_{\mathrm{LRTDDFT}}(R_{\mathrm{LRTDDFT}}) = \omega(t)$. At each time, $\omega(t)$ is computed from the field-free linear response of the molecule. Considering this $\omega(t)$ as obtained from the experiment (i.e., exact), we see that especially $R_{\mathrm{LRAEXX}}(\omega)$ does a reasonably good job except where nuclear configurations whose exact frequencies go below the AEXX minimum frequency, while $R_{\mathrm{LRALDA}}(\omega)$ has some error especially at later times as expected because of the difficulties getting long-range charge-transfer excitations correct but does a good job at earlier times. On the other hand, if RT-Ehrenfest was used to simulate the "molecular movie", both $R_{\mathrm{LRAEXX}}(\omega_{\mathrm{RTAEXX}})$ and $R_{\mathrm{LRALDA}}(\omega_{\mathrm{RTALDA}})$ are qualitatively wrong from the very start. The problem with RT-Ehrenfest is related to the spurious peak shifts that have been observed in TDDFT when the system has been driven far from a ground state.[28−31]

In summary, LR-Ehrenfest calculations perform significantly better than RT-Ehrenfest simulations when using adiabatic xc functional approximations, because the xc functional is evaluated on a domain that is closer to that from which they were derived. We note these conclusions hold for individual trajectories in the ensemble as well as for the ensemble. This affects qualitative predictions of coupled electron−nuclear dynamics in a number of applications, including time-resolved spectroscopy to probe ionic motion. Thus, LR-Ehrenfest calculations should be chosen over RT ones wherever possible. Our results concern the performance of approximate TDDFT in these two approaches, assuming both are computationally feasible, as in many cases of interest. For complex systems LR-Ehrenfest calculations may be more computationally expensive than RT-Ehrenfest, even as implementations of LR-TDDFT are available that have the same scaling and similar cost per excited state as a ground-state calculation.[32] In cases where the system size is large enough that obtaining the LR quantities is too computationally expensive, our results suggest caution: using functionals that give generally good linear response may not perform as well as expected when used in RT-Ehrenfest calculations. We should note that LR-TDDFT is known to be inaccurate for a number of situations, including double-excitations and conical intersections with the ground state. Still there is no reason to expect that RT-TDDFT will perform better in these cases. When external fields are present, LR-Ehrenfest is not as easily generalizable as RT-Ehrenfest because of requiring the explicit evaluation of matrix elements of the applied field between interacting BO states and the greater significance of coupling terms between excited states, inaccessible from linear response.[18,33−36] In a broader view, we expect some of the issues we highlighted here to be relevant in any self-consistent approach to excited-state dynamics, for example in time-dependent Hartree−Fock and orbital-dependent functional approaches. In these situations also, an LR-Ehrenfest calculation should be superior.

■ ASSOCIATED CONTENT

Supporting Information

The Supporting Information is available free of charge at https://pubs.acs.org/doi/10.1021/acs.jpclett.1c02020.

Numerical details of our calculations (PDF)

Upper panel: evolution of the nuclear trajectories for the LR and RT AEXX Ehrenfest calculations as well as the exact nuclear wave packet (see legend); lower panel: the corresponding electronic densities (MP4)

Upper panel: evolution of the nuclear trajectories for the LR ALDA and RT ALDA Ehrenfest calculations as well as the exact nuclear wave packet (see legend); lower panel: the corresponding electronic densities (MP4)

Time evolution of the electronic densities and corresponding v_s and v_{ext} potential for RT ALDA and RT AEXX; for reference, the exact electronic density is shown (MP4)

■ AUTHOR INFORMATION

Corresponding Authors

Lionel Lacombe − *Department of Physics, Rutgers University, Newark 07102 New Jersey, United States;* orcid.org/0000-0002-5535-424X; Email: liolacombe@gmail.com

Neepa T. Maitra − *Department of Physics, Rutgers University, Newark 07102 New Jersey, United States;* Email: neepa.maitra@rutgers.edu

Complete contact information is available at: https://pubs.acs.org/10.1021/acs.jpclett.1c02020

Notes

The authors declare no competing financial interest.

■ ACKNOWLEDGMENTS

Financial support from the National Science Foundation Award CHE-1940333 (N.T.M.) and from the Department of Energy, Office of Basic Energy Sciences, Division of Chemical Sciences, Geosciences and Biosciences under Award No. DESC0020044 (L.L.) are gratefully acknowledged.

■ REFERENCES

(1) Runge, E.; Gross, E. K. U. Density-Functional Theory for Time-Dependent Systems. *Phys. Rev. Lett.* **1984**, *52*, 997−1000.

(2) Marques, M. A., Maitra, N. T., Nogueira, F. M., Gross, E., Rubio, A., Eds. *Fundamentals of Time-Dependent Density Functional Theory*; Springer: Berlin, 2012; Vol. 837.

(3) Ullrich, C. A. *Time-Dependent Density-Functional Theory: Concepts and Applications*; Oxford University Press: Oxford, 2011.

(4) Maitra, N. T. Perspective: Fundamental Aspects of Time-Dependent Density Functional Theory. *J. Chem. Phys.* **2016**, *144*, 220901.

(5) Rozzi, C. A.; Falke, S. M.; Spallanzani, N.; Rubio, A.; Molinari, E.; Brida, D.; Maiuri, M.; Cerullo, G.; Schramm, H.; Christoffers, J.; et al. Quantum Coherence Controls the Charge Separation in a Prototypical Artificial Light-Harvesting System. *Nat. Commun.* **2013**, *4*, 1602.

(6) Tavernelli, I. Nonadiabatic Molecular Dynamics Simulations: Synergies between Theory and Experiments. *Acc. Chem. Res.* **2015**, *48*, 792−800.

(7) Muuronen, M.; Parker, S. M.; Berardo, E.; Le, A.; Zwijnenburg, M. A.; Furche, F. Mechanism of Photocatalytic Water Oxidation on Small TiO2 Nanoparticles. *Chem. Sci.* **2017**, *8*, 2179−2183.
(8) Draeger, E. W.; Andrade, X.; Gunnels, J. A.; Bhatele, A.; Schleife, A.; Correa, A. A. Massively Parallel First-Principles Simulation of Electron Dynamics in Materials. *J. Parallel Distrib. Comput.* **2017**, *106*, 205−214.
(9) Tancogne-Dejean, N.; Oliveira, M. J. T.; Andrade, X.; Appel, H.; Borca, C. H.; Le Breton, G.; Buchholz, F.; Castro, A.; Corni, S.; Correa, A. A.; et al. Octopus, a Computational Framework for Exploring Light-Driven Phenomena and Quantum Dynamics in Extended and Finite Systems. *J. Chem. Phys.* **2020**, *152*, 124119.
(10) Apra, E.; Bylaska, E. J.; de Jong, W. A.; Govind, N.; Kowalski, K.; Straatsma, T. P.; Valiev, M.; van Dam, H. J. J.; Alexeev, Y.; Anchell, J.; et al. NWChem: Past, Present, and Future. *J. Chem. Phys.* **2020**, *152*, 184102.
(11) Giannozzi, P.; Baseggio, O.; Bonfá, P.; Brunato, D.; Car, R.; Carnimeo, I.; Cavazzoni, C.; de Gironcoli, S.; Delugas, P.; Ferrari Ruffino, F.; et al. Quantum ESPRESSO toward the Exascale. *J. Chem. Phys.* **2020**, *152*, 154105.
(12) Noda, M.; Sato, S. A.; Hirokawa, Y.; Uemoto, M.; Takeuchi, T.; Yamada, S.; Yamada, A.; Shinohara, Y.; Yamaguchi, M.; Iida, K.; et al. SALMON: Scalable Ab-Initio Light-Matter Simulator for Optics and Nanoscience. *Comput. Phys. Commun.* **2019**, *235*, 356−365.
(13) García, A.; Papior, N.; Akhtar, A.; Artacho, E.; Blum, V.; Bosoni, E.; Brandimarte, P.; Brandbyge, M.; Cerdá, J. I.; Corsetti, F.; et al. Siesta: Recent Developments and Applications. *J. Chem. Phys.* **2020**, *152*, 204108.
(14) Car, R.; Parrinello, M. Unified Approach for Molecular Dynamics and Density-Functional Theory. *Phys. Rev. Lett.* **1985**, *55*, 2471−2474.
(15) Tully, J. C. Mixed Quantum-Classical Dynamics. *Faraday Discuss.* **1998**, *110*, 407−419.
(16) Parker, S. M.; Rappoport, D.; Furche, F. Quadratic Response Properties from TDDFT: Trials and Tribulations. *J. Chem. Theory Comput.* **2018**, *14*, 807−819.
(17) Bowman, D. N.; Asher, J. C.; Fischer, S. A.; Cramer, C. J.; Govind, N. Excited-State Absorption in Tetrapyridyl Porphyrins: Comparing Real-Time and Quadratic-Response Time-Dependent Density Functional Theory. *Phys. Chem. Chem. Phys.* **2017**, *19*, 27452−27462.
(18) Parker, S. M.; Roy, S.; Furche, F. Multistate Hybrid Time-Dependent Density Functional Theory with Surface Hopping Accurately Captures Ultrafast Thymine Photodeactivation. *Phys. Chem. Chem. Phys.* **2019**, *21*, 18999−19010.
(19) Lacombe, L.; Suzuki, Y.; Watanabe, K.; Maitra, N. T. Electron Scattering in Time-Dependent Density Functional Theory. *Eur. Phys. J. B* **2018**, *91*, 96.
(20) Helbig, N.; Fuks, J. I.; Casula, M.; Verstraete, M. J.; Marques, M. A. L.; Tokatly, I. V.; Rubio, A. Density Functional Theory beyond the Linear Regime: Validating an Adiabatic Local Density Approximation. *Phys. Rev. A: At., Mol., Opt. Phys.* **2011**, *83*, 032503.
(21) Casula, M.; Sorella, S.; Senatore, G. Ground State Properties of the One-Dimensional Coulomb Gas Using the Lattice Regularized Diffusion Monte Carlo Method. *Phys. Rev. B: Condens. Matter Mater. Phys.* **2006**, *74*, 245427.
(22) Maitra, N. T. Charge Transfer in Time-Dependent Density Functional Theory. *J. Phys.: Condens. Matter* **2017**, *29*, 423001.
(23) Petersilka, M.; Gossmann, U. J.; Gross, E. K. U. Excitation Energies from Time-Dependent Density-Functional Theory. *Phys. Rev. Lett.* **1996**, *76*, 1212−1215.
(24) Grabo, T.; Petersilka, M.; Gross, E. K. U. Molecular Excitation Energies from Time-Dependent Density Functional Theory. *J. Mol. Struct.: THEOCHEM* **2000**, *501*−*502*, 353−367.
(25) Pertot, Y.; Schmidt, C.; Matthews, M.; Chauvet, A.; Huppert, M.; Svoboda, V.; von Conta, A.; Tehlar, A.; Baykusheva, D.; Wolf, J.-P.; et al. Time-Resolved X-Ray Absorption Spectroscopy with a Water Window High-Harmonic Source. *Science* **2017**, *355*, 264−267.
(26) Attar, A. R.; Bhattacherjee, A.; Pemmaraju, C. D.; Schnorr, K.; Closser, K. D.; Prendergast, D.; Leone, S. R. Femtosecond X-Ray Spectroscopy of an Electrocyclic Ring-Opening Reaction. *Science* **2017**, *356*, 54−59.
(27) Toulson, B. W.; Borgwardt, M.; Wang, H.; Lackner, F.; Chatterley, A. S.; Pemmaraju, C. D.; Neumark, D. M.; Leone, S. R.; Prendergast, D.; Gessner, O. Probing Ultrafast C-Br Bond Fission in the UV Photochemistry of Bromoform With Core-to-Valence Transient Absorption Spectroscopy. *Struct. Dyn.* **2019**, *6*, 054304.
(28) Fuks, J. I.; Luo, K.; Sandoval, E. D.; Maitra, N. T. Time-Resolved Spectroscopy in Time-Dependent Density Functional Theory: An Exact Condition. *Phys. Rev. Lett.* **2015**, *114*, 183002.
(29) Luo, K.; Fuks, J. I.; Maitra, N. T. Studies of Spuriously Shifting Resonances in Time-Dependent Density Functional Theory. *J. Chem. Phys.* **2016**, *145*, 044101.
(30) Habenicht, B. F.; Tani, N. P.; Provorse, M. R.; Isborn, C. M. Two-Electron Rabi Oscillations in Real-Time Time-Dependent Density-Functional Theory. *J. Chem. Phys.* **2014**, *141*, 184112.
(31) Provorse, M. R.; Isborn, C. M. Electron Dynamics with Real-Time Time-Dependent Density Functional Theory. *Int. J. Quantum Chem.* **2016**, *116*, 739−749.
(32) Furche, F.; Krull, B. T.; Nguyen, B. D.; Kwon, J. Accelerating Molecular Property Calculations with Nonorthonormal Krylov Space Methods. *J. Chem. Phys.* **2016**, *144*, 174105.
(33) Li, Z.; Liu, W. First-Order Nonadiabatic Coupling Matrix Elements between Excited States: A Lagrangian Formulation at the CIS, RPA, TD-HF, and TD-DFT Levels. *J. Chem. Phys.* **2014**, *141*, 014110.
(34) Li, Z.; Suo, B.; Liu, W. First Order Nonadiabatic Coupling Matrix Elements between Excited States: Implementation and Application at the TD-DFT and pp-TDA Levels. *J. Chem. Phys.* **2014**, *141*, 244105.
(35) Zhang, X.; Herbert, J. M. Analytic Derivative Couplings in Time-Dependent Density Functional Theory: Quadratic Response Theory versus Pseudo-Wavefunction Approach. *J. Chem. Phys.* **2015**, *142*, 064109.
(36) Ou, Q.; Bellchambers, G. D.; Furche, F.; Subotnik, J. E. First-Order Derivative Couplings between Excited States from Adiabatic TDDFT Response Theory. *J. Chem. Phys.* **2015**, *142*, 064114.

https://doi.org/10.1021/acs.jpclett.1c02020
J. Phys. Chem. Lett. 2021, 12, 8554−8559